Finite Element based Fatigue Crack Growth Simulations in Featured Plate Specimens

A.M. Gilmartin, M.B. Henderson*, T.J.W. Ward, B. Vermeulen

QinetiQ, Cody Technology Park, Farnborough, Hampshire GU14 0LX, United Kingdom
*ALSTOM Power Tech. Centre, Whetstone, Leicester LE8 6LH, United Kingdom

Gas turbine engine combustor manufacturers face the challenge of achieving improved efficiency against the increasingly stringent regulations concerning NO_x emissions. Revolutionary changes in design styles will be required with the increased use of high stress concentration features such as effusion cooling holes. Lifetime prediction for new combustor designs will require an estimation of life to first crack and an estimation of the crack propagation life. This paper studies crack propagation in featured low cycle fatigue specimens intended to simulate cooling holes within a combustor liner wall. Based on extensive fatigue crack growth testing of corner notch specimens, linear elastic fracture mechanics crack growth laws have been postulated for the γ' strengthened, nickel-based superalloy C263 at 300 and 800°C. These laws have been used to predict the growth rates for cracks growing within featured specimens and the results compared with data obtained from experimental testing of specimens with 90° holes. Direct comparison with growth rates obtained from load-controlled fatigue testing of the specimens at 300 and 800°C has shown the growth laws to provide good predictions for the behaviour of the material in the vicinity of the feature. The meshing of the test specimens with elliptical and straight through cracks was performed with the aid of ZENCRACK software, which provides singular elements to a conventional mesh. The 3-D analysis was performed using ABAQUS Standard.

1. Introduction

Due to the continued drive for improved performance commensurate with reduced component life costs, future generation combustors will be expected to perform with increased levels of efficiency whilst minimizing the emissions of harmful NO_x toxins into the environment. Achieving such demanding goals will require higher combustion temperatures and consequently more sophisticated cooling techniques. However, advanced cooling techniques, such as plain and angled effusion cooling holes, add more stress concentrating features into the combustor. With the introduction of such design features it is essential to have a thorough understanding of the behavior of the material in the vicinity of the feature itself in order to preserve the safety and integrity of the component. To calculate the service lifetime of a combustor, the number of engine cycles until crack initiation needs to be estimated. Beyond this point the crack growth rate is the key parameter, as it determines the inspection intervals that can safely be adopted. A series of analyses was undertaken to model the fatigue crack growth behavior of a featured plate specimen, containing a central vertically aligned laser-drilled hole, at 90° to the specimen surface. The specimens were made from the γ' strengthened, nickel-based superalloy C263, a material used by aero-engine manufactures.

The objective of this work was to establish the validity of fatigue crack growth laws proposed for C263, as derived from fatigue crack growth testing of corner notched (CN) specimens, in modeling fracture about combustor cooling holes.

In the paper fatigue test results for CN specimens are used to develop linear elastic fatigue crack growth models at different temperatures. These models relate the crack growth rate to the stress intensity factor for the given geometry. The models are then applied to specimens featuring cooling holes used in combustors. The finite element mesh generation for these featured specimens including a propagation crack front is presented. The mesh is used to analyze the stress intensity in front of the crack tip. A geometry correction function derived from these analyses allows a comparison of model predictions with the experimental data. A discussion of the derived results concludes the paper.

2. Fatigue Crack Growth Modelling

Fatigue crack growth laws for the nickel based super alloy have been proposed by Henderson and Wilcock, (Henderson, 2001) at 300 and 800°C based upon data obtained from an expansive baseline test programme of corner notched specimens at various R_σ ratios. The laws proposed are based on the Paris equation (Paris, 1961) and incorporate the linear elastic fracture mechanics parameter ΔK. To accommodate the effects of R_σ ratio the Walker correction method (Walker, 1970) was applied to ΔK values of the CN specimens to determine an effective ΔK_{eff}:

$$\Delta K_{\text{eff}} = \Delta K(1-R_\sigma)^{n_{\text{W}}-1}, \tag{1}$$

where n_w is the Walker correction parameter. Although, creep damage is likely to exist ahead of the crack tip at 800°C it has been assumed to be negligible for the featured specimens and consequently the crack growth model is based on Plastic-Plastic (PP) cyclic tests with no dwell periods. Application of the Walker correction method to the determined ΔK values for each data set was found to correlate the effects of R_σ ratio with minimal scatter observed in the data. Statistical analyses of each data set enabled the determination of mean gradients and intercept values to be defined such that the following mean fatigue crack growth behavior model were proposed for C263 at 300 and 800°C using the Paris equation:

$$\frac{da}{dN} = C(\Delta K_{\text{eff}})^m, \tag{2}$$

where ΔK_{eff} is given by Equation 1. The temperature dependent values of the parameters C, m and n_{W} are given in Table 1. The parameter values C_{min} and C_{max} also in Table 1 define a scatter band between a minimum and maximum crack growth rate at each temperature. The width of the scatter bands was determined as maximum and minimum limits of the Walker-corrected fatigue crack growth data. A fuller statistical analysis to determine the +/- 3 standard deviation limits has yet to be completed.

3. Application to the Cooling Hole Geometry

To simulate the thermal and mechanical conditions around a cooling hole in a combustion chamber in a laboratory testing facility, plane and featured specimens have been designed and tested. Featured low cycle fatigue specimens containing a central hole orientated perpendicular to its upper and lower surfaces were tested. The dimensions of the hole (diameter 0.7mm) have been designed to be representative of typical cooling holes found in real aero-engine combustors.

To determine the stress intensity fields ahead of an advancing crack profile it is necessary to perform a series of finite element stress analyses. Cracking within the specimen was considered most likely to occur in two distinct phases and models were created to simulate each phase.

Phase 1: Crack initiation was assumed to occur in the middle of the hole in the plain perpendicular to the direction of the load, as shown schematically in Figure 1a. Due to the variation in the stress field ahead of the feature it was anticipated that crack growth would mainly occur along the highest stress concentration, i.e. along the length of the hole (vertical), and not into the bulk of the material (horizontal). An idealized elliptical crack front was created with a 2:1 length ratio with respect to the major and minor axes of the ellipse. Six meshes were created to model an advancing elliptical crack front, with length ratios kept constant at 2:1. At the point of penetration with the upper and lower surfaces of the specimen the crack morphology was considered to be no longer representative of a real crack behavior and a new model was adopted (Phase 2).

Phase 2: With the outer flanks of the elliptical crack front penetrating the specimens' upper and lower surfaces a modified crack morphology was adopted and modeled. Examination of the various specimen fracture surfaces had shown through cracks with crack fronts penetrating entire specimen cross-sections. Although each of the observed crack fronts appeared to show signs of curvature, a simplification was made during modeling with each crack assuming a linear profile as shown in Figure 1b. Nine meshes were created to model an advancing through crack across a range from approximately 0.5 to 5mm which is similar to the surface crack lengths observed during specimen testing.

Meshing of the various models was carried out using the pre-processing package FEMSYS (FEMSYS, 1997) in tandem with the specialist fatigue crack software ZENCRACK (Zentech, 1998). ZENCRACK is designed to introduce cracks into existing meshes. By automatically substituting specialist elements or 'crack blocks' into standard meshes the programme enables the user to generate and model various crack configurations. Two types of crack block are offered (Figure 2) with quarter circular and through crack morphologies. Each crack block is designed to be compatible with one another so that numerous potential crack geometries can be modeled. For this study two 'uncracked' meshes were constructed using standard 20 noded elements one for elliptical and one for through cracks. Due to symmetry conditions within each of the specimens and in an effort to optimize computational times 1/8th portions of each specimen were modeled as highlighted in Figure 1. The crack was modeled by selecting a group of elements in the FE mesh at the front of the crack and substituting a crack block for each element. Figures 3 and 4 show typical meshes produced during modeling of each crack growth phase.

All analyses were performed using the finite element software package ABAQUS v5.8. ABAQUS (Hibbitt, 1998) characterizes the energy release rate associated with the extension of a crack by calculating the contour integral J (Rice, 1974). A J value was determined for each crack model by averaging the values obtained over four contours around the crack tip.

The parameter *J* is primarily used to model fracture within materials behaving non-linearly, however, when linear elastic material behavior is assumed, as in the case of this study, *J* is equivalent to the strain energy release rate *G* (Hertzberg, 1996). As the energy parameter *G* can be related directly to the stress intensity factor *K* (Ashby, 1993) a corresponding relationship can be established between *J*, *K* and the Young's modulus *E*:

$$J = G = \frac{K^2}{E'} \text{ with } \quad E' = \begin{cases} E & (\text{plane stress}) \\ \dfrac{E}{1\text{-}\nu^2} & (\text{plane strain}) \end{cases}, \tag{3}$$

where in this study the plane strain assumption has been adopted.

4. Experiments

To validate the predictions of the fatigue crack growth model Equation 2 applied on cooling holes, LCF tests using featured specimens were undertaken. The tests were conducted at 300 and 800°C using a PP load-controlled trapezoidal cycle (0.2s:0.2s:0.2s:0.2s) for a range of maximum stresses. The test matrix detailing temperature, loading conditions and results is shown in Table 2. All tests were performed at an R_σ ratio = 0 with ramp times of 0.2s. Test conditions were chosen to replicate those found at common failure sites within combustors. Fracture within the specimen was measured using a direct current potential drop (DCPD) technique (Hicks, 1982).

From the DCPD recording the relationship between crack length and number of cycles can be derived and the derivative *da/dN* can be calculated. However, to compare the test results with the model predictions for the C263 CN specimen database, the change in stress intensity factor ΔK experienced by the specimen, is required. The stress intensity factor can be related directly to the crack length *a* (Rice, 1985) by introducing a geometry correction function *F(a)*, which depends on the given specimen geometry:

$$\Delta K = F(a) \cdot \Delta\sigma\sqrt{\pi\, a} \tag{4}$$

where $\Delta\sigma$ is the applied stress range. The geometry correction function was derived from Equation 4 by calculating supporting points of the function *F(a)* using the ΔK values from the FE analyses for each of the nine crack lengths for which a crack mesh was generated. A sixth order polynomial fit through the supporting points was used to create a continuous function. The geometry correction function *F(a)* is shown in Figure 5. Once a geometry correction function *F(a)* is established for a given specimen geometry the experimental change in stress intensity ΔK can be calculated using Equation 4 for any crack length. Note, that in the case of an R_σ ratio = 0 the Walker correction, Equation 1, is the identity function and $\Delta K_{\text{eff}} = \Delta K$. The featured specimen experimental data are summarised in logarithmic plots of *da/dN* versus ΔK_{eff} and are shown in Figure 6 and 7 for 300 and 800°C, respectively. The model Equation 2 predictions at these temperatures, together with their maximum and minimum limits, are included in the figures.

After crack initiation, inspection intervals have to be calculated based on the number of cycles for the crack to grow to a given length. To do this the model for the crack growth rate, Equation 2, was integrated over the number of cycles:

$$N = \frac{1}{C} \int_{r}^{r+a} \Delta K_{\text{eff}}^{-m} \, da \,, \tag{5}$$

where r is the radius of the hole through the specimen. The change in stress intensity ΔK is calculated using Equation 4, employing the continuous polynomial fit for the geometry correction function $F(a)$. This allows crack lengths other than those modelled using FE to be considered.

5. Results

Figure 6 compares directly the fatigue crack growth rate data generated at 300°C for featured specimen tests #131101 and #191101 with the predicted maximum, mean and minimum growth rate data. Distinctly different m and C values (ie., the gradient and intercept for the da/dN vs ΔK_{eff} curve) have resulted for the featured specimen tests compared with the predictions based on CN data generated at 300°C. For the case of test #191101 the steady state regime of crack growth lies within the bounds of the CN specimen database. However, in the case of test #131101 the crack growth rate lies marginally above the line representing the maximum fatigue crack growth. With the scarcity of featured specimen data at 300°C, it is difficult to assess confidently the validity of the proposed growth laws in modelling fatigue in these features at this temperature.

A comparison of the database model with the featured specimen data at 800°C is depicted in Figure 7. For these tests similar m and C values have resulted for the featured specimen tests to those used in the model (Table 1) and reasonably good agreement is found. Of the five tests, three lie within the bounds defined by the mean and maximum crack growth rates. Only two of the tests deviate beyond the maximum limit. For test #221101 this might be caused by the reuse of a specimen run out at 300°C.

The duration between crack initiation and failure of the specimens was predicted using Equation 5 with the final crack length in the upper integration limit. Table 3 shows the predicted crack propagation for each test in comparison with the experimental results. The results are represented graphically in Figure 8 with difference factors, which are the predicted propagation phases divided by the actual propagation phases. This shows the amount by which the model over or under predicts the experimental results. In the case of tests performed at 300°C the integral, Equation 5, consistently over predicts the duration of the crack propagation phase. Predictions are between two and three times greater than that recorded during the featured specimen tests. For the 800°C data the integral gives a much better approximation of the growth phase within each of the specimens. Four of the five growth phase predictions are conservative with difference factors ranging from 0.6 to 0.9. However, the re-used specimen #221101 deviates by 1.9 times from the growth prediction.

6. Conclusions

A study has been conducted to establish the effectiveness of fatigue crack growth laws in characterizing fatigue in the vicinity of combustor cooling holes for the nickel superalloy C263 material. Analyses have focused upon a featured specimen containing a central hole, aligned perpendicular to its upper and lower surfaces, with dimensions representative to that of a typical component cooling hole.

A load-controlled LCF test programme has been undertaken with featured specimens at 300 and 800°C. The results of the testing have been used to benchmark the predictions due to a fatigue crack growth database model for C263. Crack growth within C263 has been characterized using the linear elastic fracture mechanics parameter. A series of finite element analyses have been constructed to model an advancing crack front through the specimen.

Direct comparison between the predicted fatigue crack growth rates at 300 and 800°C has produced mixed results. At 300°C the models appear to be non-conservative with growth predictions two to three times greater than those observed during testing. The lack of featured specimen data at 300°C has restricted the analysis somewhat. It is clear, however, that the 300°C featured specimen data lie upper bound for much of the fatigue crack growth curve (Figure 6), but have a shallower slope than the predicted lines so that the curves cross the model. The consequence is that the model over predicts the crack growth life for the featured specimens. This may be attributable to differences between the dominant stress states found for CN and centre-crack panel type specimens not accounted for in the FE analysis conducted; the T-stress terms (Rice, 1974) for CN specimens are distinctly different to those for through crack specimens and impact on the crack growth rates observed.

At 800°C five tests were completed successfully with three showing close agreement with rates predicted by the proposed growth law. At 800°C the life predictions are conservative with results close to the experimental results. The reasons for the poor agreement at 300°C and good agreement at 800°C are unclear at present, though this may be associated with differences in crack propagation mechanism in C263 at the two temperatures.

7. References

1. Henderson, M. B. and Wilcock I. M., "CPLIFE Report R11: Modelling the Fatigue Crack Growth Behaviour of the Combustor Alloy C263", QinetiQ Report QINETIQ/FST/SMC/TRO11169, 2001.

2. Paris, P. C, Gomez, M.P. and Anderson, W. E., "A rational analytical theory of fatigue", The Trend in Engineering 13, 1961, pp. 9-14.

3. Walker, K., "The effect of stress ratio during crack propagation and fatigue for 2024-T3 and 7055-T6 aluminium", In Effects of Environment and Complex Load History for Fatigue Life, Special Technical Publication 462, pp. 1-14, Philadelphia: American Society for Testing and Materials, 1970.

4. FEMSYS Engineering Software, "FEMGV: User Manual", Version 5, 1997.

5. Zentech International Ltd., "ZENCRACK: User Manual & Installation and Execution Manual", Issue 6, 1998.

6. Hibbitt, Karlsson & Sorensen, Inc., “ABAQUS User Maual”, Version 5.8, 1998.

7. Rice, J. R., “Limitations to the small scale yielding approximation for crack tip plasticity”, Journal of Mechanics and Physics of Solids 22, 1974, pp. 17-26.

8. Hertzberg, R. W., “Deformation and Fracture Mechanics of Engineering Materials”, J. W. Wiley & Sons, 1996, p. 361.

9. Ashby, M.F. and Jones D. R. H., “Engineering Materials 1”, Pergamon, 1993, p. 215.

10. Hicks M. A. and A.C. Pickard, “A comparison of theoretical and experimental methods of calibration the electrical potential drop technique for crack length determination”, Int. Journal of Fracture 20, 1982, pp. 91-101.

11. Rice, J.R., “First order variations in elastic fields due to variation in location of a planar crack front”, Journal of Applied Mechanics 52, 1985, pp. 571-579.

8. Tables

Table 1: Summary of the Walker corrected parameters at 300 and 800°C.

Temperature [°C]	*C* [m/cycle]			*m*	n_W
	max	min	mean		
300	3.5644E-14	8.7492E-15	1.7659E-14	4.3815	0.38
800	1.8958E-09	8.6729E-10	1.2822E-09	1.8349	0.45

Table 2: Test matrix of the featured specimen test programme.

Test	Temp. [°C]	Max Stress	Cycles To Initiation	Cycles To Failure
#191101	300	350	67200	184067
#131101	300	400	40000	93345
#201101	800	300	91950	101506
#181101	800	350	12000	20952
#211101	800	375	5300	11097
#141101	800	400	4650	10058
#221101*	800	500	750	2050

*Restart of a specimen run out at 300°C.

Table 3: Crack growth phase predictions compared against experimental results.

Test	Temp. (°C)	Applied Stress (MPa)	Crack length @ failure (af) (mm)	No. of cyles to initiation (Ni) (mm)	Number of cycles to failure (Nf)	Propagation Phase	Predicted Propagation phase	Difference Factor
#131101	300	375	2.25	40,000	93,345	53,345	157,748	2.96
#191101	300	330	2.33	67,200	184,067	116,867	276,918	2.37
#221101	800	482	1.64	750	2,050	1,300	2522	1.94
#141101	800	393	2.56	4,650	10,058	5,408	4553	0.84
#211101	800	365	2.3	5,300	11,097	5,797	4989	0.86
#181101	800	342	2.265	12,000	20,952	8,952	5586	0.62
#201101	800	292	1.6	91,950	101,506	9,556	6372	0.67

9. Figures

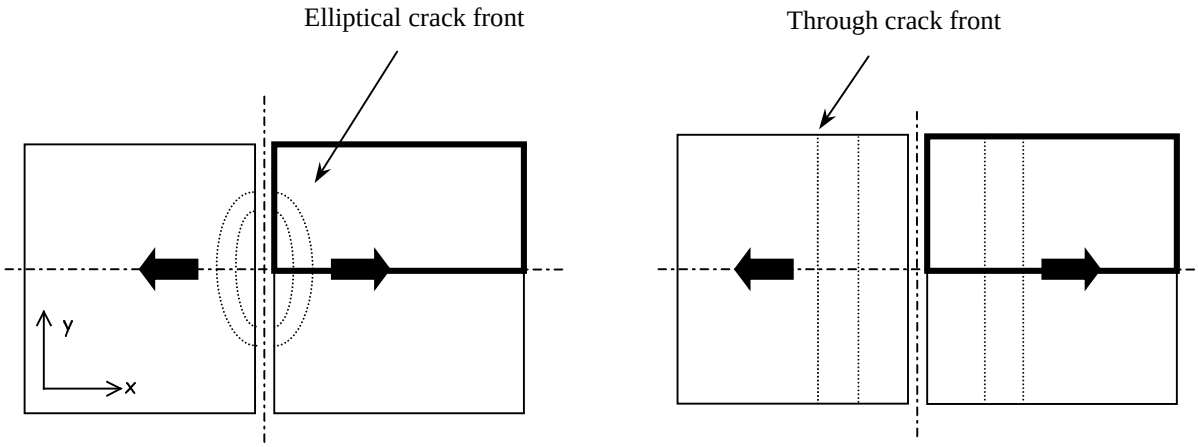

Figure 1: Featured specimen x-section showing crack morphologies incorporated (1/8th models used in FE study – highlighted in red).

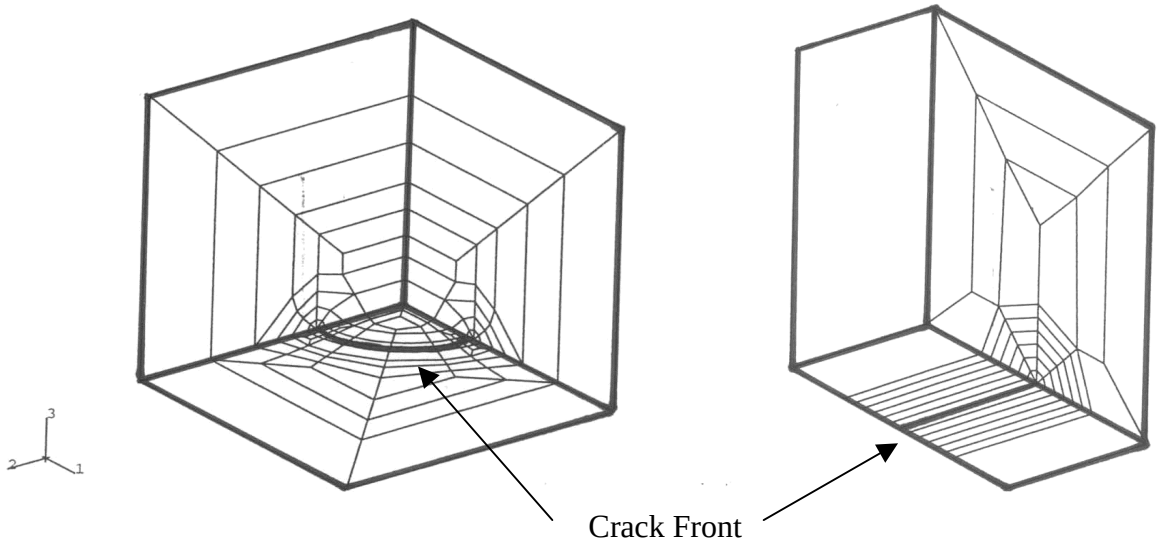

Figure 2: Crack blocks incorporated into the software package ZENCRACK.

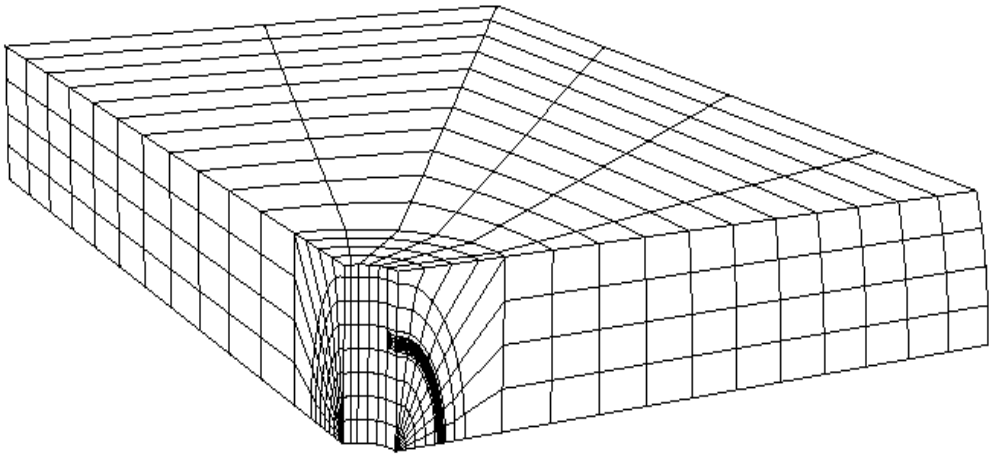

Figure 3: FEM generated to model phase 1 cracking (crack front located where elements are concentrated).

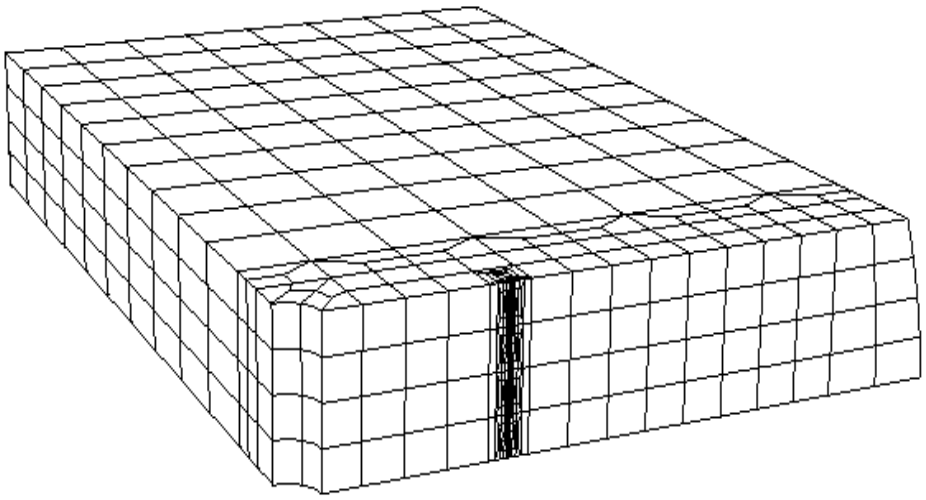

Figure 4: FEM generated to model phase 2 cracking (crack front located where elements are concentrated).

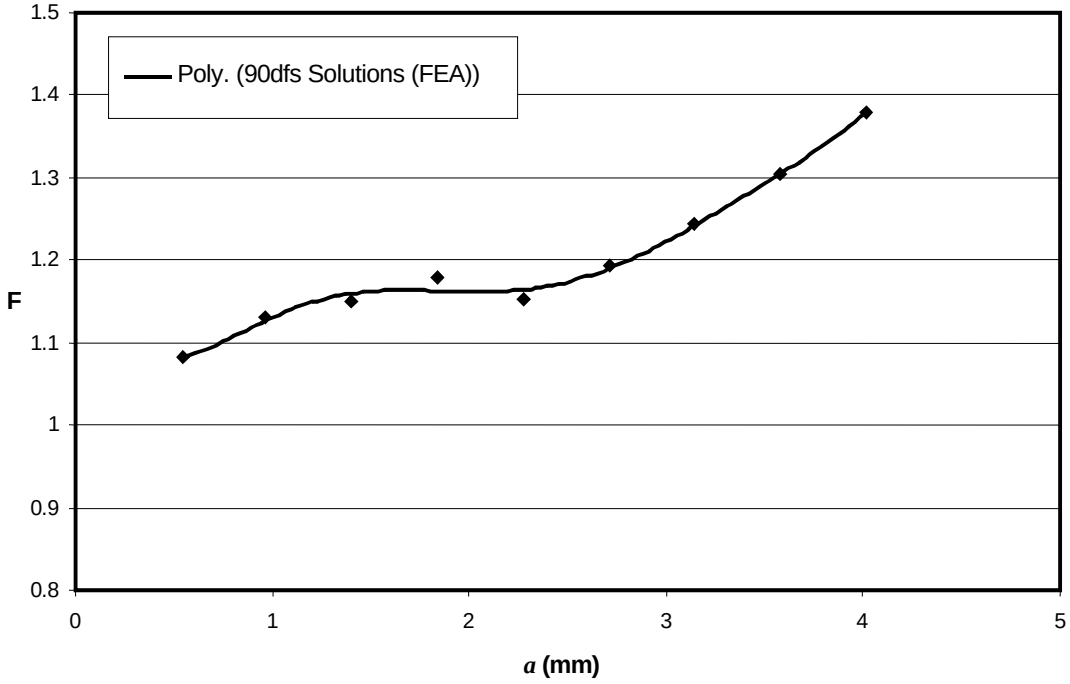

Figure 5: Geometry correction function *F(a)* for the featured specimen.

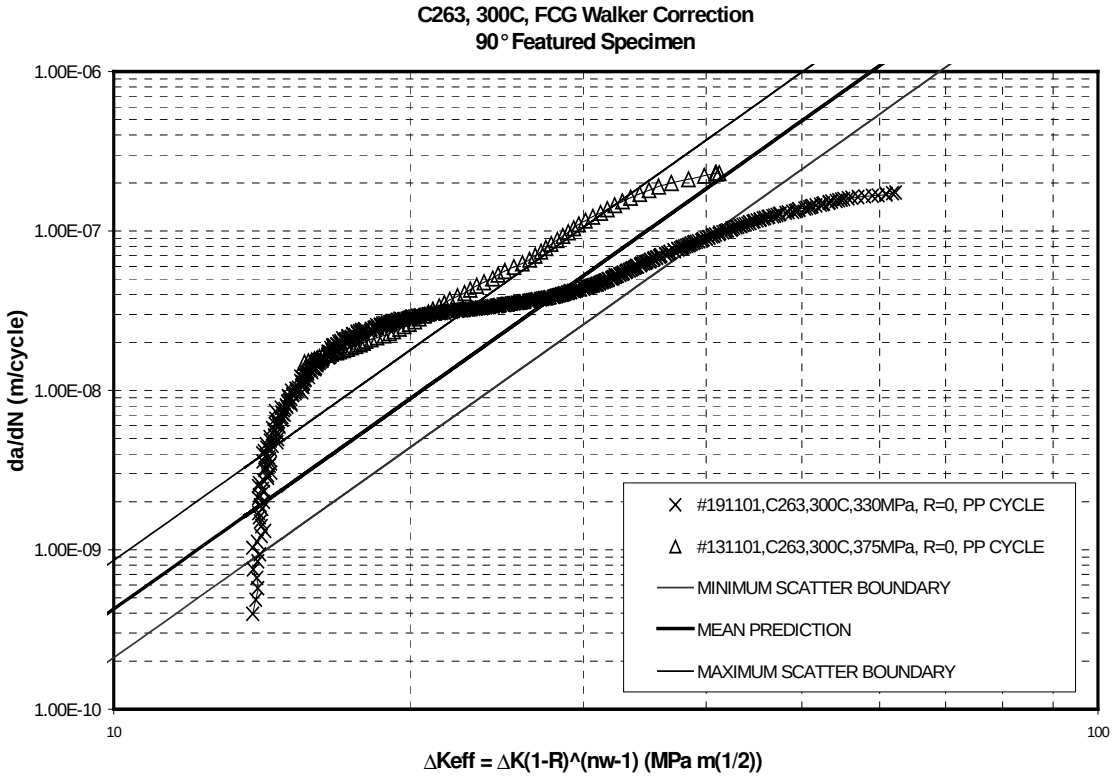

Figure 6: Comparison between the featured specimen and model fatigue crack growth rates at 300°C.

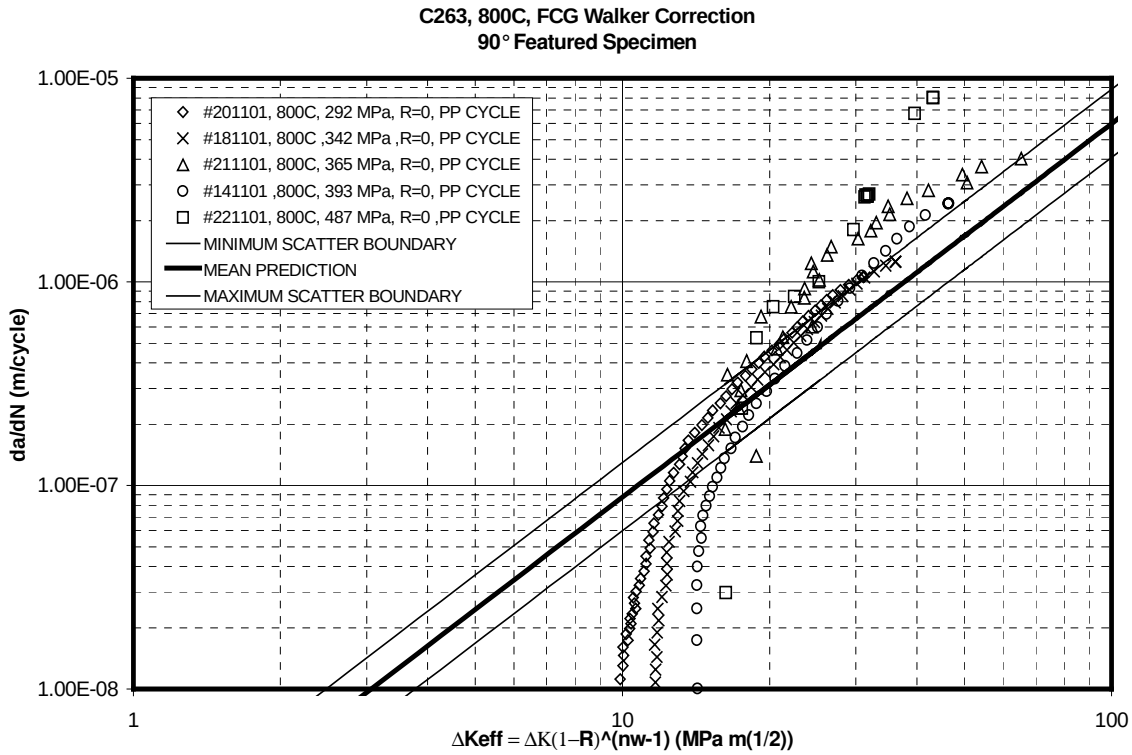

Figure 7: Comparison between the featured specimen and model fatigue crack growth rates at 800°C.

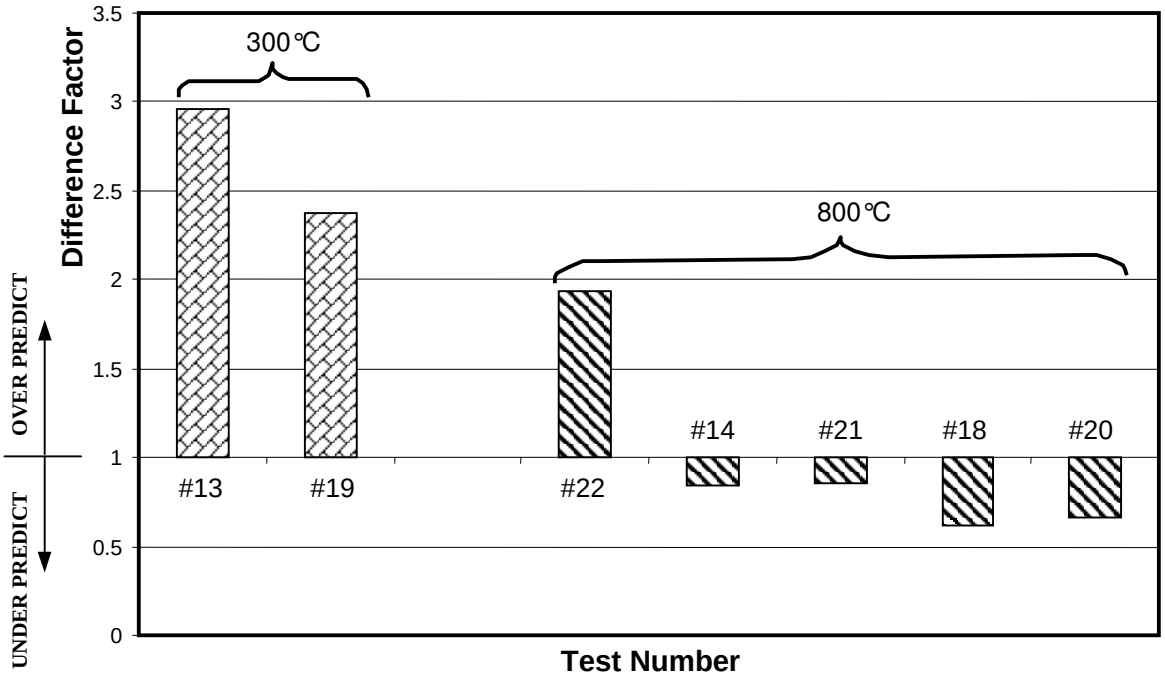

Figure 8: Comparison between predicted and actual crack growth (difference factor = predicted propagation/actual propagation).

10. Acknowledgment

This work has been performed within the Brite EuRam III programme CPLIFE.

BE97-4034 (1997-2001) supported by EC Brussels. The project partners are: Rolls-Royce UK (co-ordinator), Alstom Power S, CNR-TeMPE I, Fiat Avio I, JRC Petten NL, MTU D, *QinetiQ* UK, Rolls-Royce D, Sener E and Turbomeca F.